Advances in Environmental Technology 3 (2017) 139-149

Advances in Environmental Technology

journal homepage: http://aet.irost.ir

Adsorption of Cesium, Strontium, and Rubidium radionuclides in the Mag-molecular process: The influence of important factors

Fatemeh Tangestani[1], Mohammad Hasan Mallah[2], Abbas Rashidi[1*], Rohollah Habibzadeh,[2]

[1]Department of Chemical Engineering, Faculty of Engineering, University of Mazandaran, Babolsar, Iran

[2] Nuclear Fuel Cycle Research School, Nuclear Science and Technology Research Institute, Tehran, Iran

A R T I C L E   I N F O

Article history:
Received 7 November 2016
Received in revised form
15 August 2017
Accepted 25 August 2017

Keywords:
Cesium
Ferritin
Strontium
Rubidium
Magmolecular process

A B S T R A C T

In this study, the adsorption of cesium, strontium, and rubidium radionuclides by ferritin magmolecules in a batch system was investigated under different experimental conditions. The experiments were conducted in a pilot plant that involved the contactor unit and the magnetic separator unit. The impact of the pollutant concentrations, adsorbent concentration, and pH on the efficiency of the process were investigated thoroughly. The maximum recovery of radionuclides in the studied domain were 57.05%, 85.42% and 71.82% for Cs^+, Sr^{2+} and Rb^+ ,respectively, in which the pollutant concentration was 363.63 mg/l, the adsorbent concentration was 0.011 g/l, and the pH was 7.5. The results showed that the ferritin adsorbent in the magmolecular process manifested a higher efficiency in adsorbing the bivalent ions of strontium compared to the univalent ions of cesium and rubidium. Furthermore, the results were statistically analyzed and the model and residual plots of each radionuclide were presented. The results also signified relationships between the independent variables and recovery.

1. Introduction

Various activities such as nuclear research reactors, the use of radioisotopes, and the production and use of radiopharmaceuticals are involved in the spread of radioactive wastes. Cesium, strontium, and rubidium are among the elements found in these wastes. These radionuclides are biologically toxic and of great importance due to their long-lasting nature and high solubility in aqueous systems [1]. Therefore, it is essential to study different treatment methods and identify an efficient, economic method that can be used in the nuclear industry. A range of different physicochemical methods including chemical precipitation, ion exchange, adsorption, membrane separation, etc. are used to eliminate radionuclides from aqueous solutions [2]. Among these methods, adsorption is a widely-used technique that is effective in eliminating pollutants from wastewater. A summary of various studies related to Cs^+, Sr^{2+}, and Rb^+ adsorption are introduced in Table 1. One adsorption technique is the use of magnetite nanoparticles [10]. Ferritin is a magnetic molecule (magmolecule) which has a spherical shell and 24 peptides with a diameter of 13 nanometer and is shown in Figure 1 [11]. The morphology of the ferritin as an adsorbent material has been indicated. X-ray structures of its shell have been known since the 1980s, and show that ferritin molecules in different mammals have very similar structures [12]. The iron in the ferritin core is stored in a cage with the inner diameter of 8 nanometer which may adsorb cesium, strontium, and rubidium. With the aid of magnetic nanoparticles (MNPs) and ionic liquids, the magmolecular process was used to adsorb the ions of selenium, antimony, uranium, etc. [13, 14]. Furthermore, functionalized magnetite nanoparticles were used to adsorb cesium and strontium radionuclides through the dialysis process [15]. As revealed from studies carried out on the adsorption of cesium, strontium, and rubidium radionuclides via various adsorbents, the most frequent and important variables to be investigated included pollutant concentrations, time, temperature,

*Corresponding author. Tel: +981135302903
E-mail address: rashidi@umz.ac.ir
DOI: 10.22104/AET.2017.577

adsorbent concentration, and pH. In this study, the impact of the variables of the initial concentration of the radionuclide, adsorbent concentration, and pH on the adsorption of cesium, strontium, and rubidium in the process of adsorption via magnetic nanoparticles was investigated.

Table 1. Summary of various reports on Cs^+, Sr^{2+}, and Rb^+ adsorption

Recovery of	Adsorbent	Variables/Studied parameters	Results	Reference
Cs^+ and Sr^{2+}	various zeolites (type A, Na-P_1, faujasite X, faujasite Y, and mordenite)	the impact of coexistent cations of sodium and potassium	The presence of the coexistent cations had no impact on the adsorption of cesium and the maximum amount of cesium and strontium adsorption were 96 and 99 percent respectively	[3]
Cs^+ and Sr^{2+}	zeolite Y nanoparticles	time (10 to 120 minutes), temperature (23 to 28 ˚C), the initial concentration of metal ion (50 to 500 mg/l), and pH (5 to 11)	maximum percent of adsorption occurred in 10 minutes, temperature of 23 ˚C, initial concentration of 50 mg/l, and pH of 11	[4]
Cs^+ and Sr^{2+}	electrocoagulation(anode: aluminum, iron, and magnesium; cathode: galvanized iron with zinc)	pH (2 to 12), current density (0.0 to 0.08 A dm^{-2}), temperature (58 to 62 ˚C) and inter-electrode distance (0.002 to 0.012 m)	maximum degree of cesium and strontium adsorption were 96.8 and 97 percent respectively under the conditions of magnesium anode, density of 0.08 A dm^{-2}, pH of 7, and inter-electrode distance of 0.003 m	[5]
Rb^+ and Cs^+	ammonium molybdophosphate-calcium alginate (AMP-NaALG)	initial concentration of rubidium and cesium, ionic strength, and temperature	cesium and rubidium's maximum adsorption (0.69 and 0.58 mmol/g respectively) occurred in the pH range of 3.5 to 4.5 and the amount was increased with a raise in the metal ion's initial concentration and decreased after a raise in the temperature and ionic strength	[6]
Cs^+	zirconia powder	temperature (23 to 58 ˚C), contact time (10 to 120 minutes), and pH (2 to 10)	the maximum amount of adsorption occurred under the temperature of 58 ˚C, time of 30 minutes, and pH of 10	[7]
Cs^+	sodium and calcium alginics	contact time (0 to 120 minutes), metal ion's initial concentration (0 to 500 mg/l), and pH (2 to 6)	maximum Cs^+ adsorption(80.64 mg/ g) occurred in a time period of 60 minutes, initial concentration of 500 mg/l, and pH of 6	[8]
Rb^+	defunctionalized and functionalized with 2-mercaptothiazoline (MTZ) and 2-mercaptobenzimidazole (MBI) imogolite hybrid surface	functional group	maximum adsorption (0.30 mmol/ g) occurred by IMO_{MTZ}	[9]

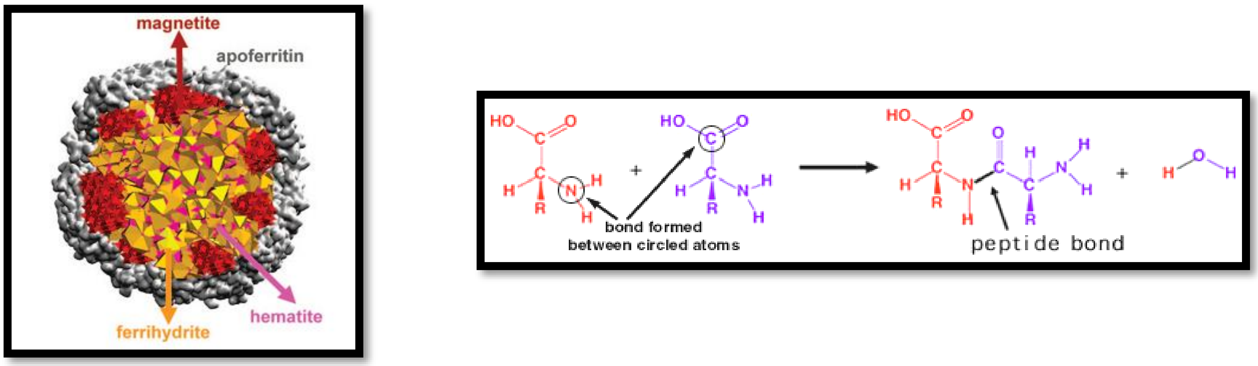

Fig. 1. The structure of ferritin

2. Materials and methods

2.1. Chemical Materials

The ferritin solution supplied by the Aldrich Chemical Co. was used in all the experiments. The water used in the experiments was distilled twice. Synthetic solutions of cesium, strontium, and rubidium were prepared by solving $CsNO_3$, $Sr(NO_3)_2$, and RbCl sourced from the Merck Chemical Co. in double-distilled water. The solution pH was adjusted by adding a small amount of the HCl or NaOH provided by the Merck Company. One gram of ferritin was kept in a container with the volume of 0.015 L which, for the preparation, was solved in 10 L of distilled water resulting in the stock solution of 0.1 g/l which would be diluted when required.

2.2. Analyses

In this study, the presented functional groups on the ferritin surface were analyzed within the wavelength range of 500 to 4000 cm^{-1} via Fourier transmission infrared spectroscopy (FTIR analysis) using the Bruker VECTOR22 model produced in Germany. To determine the radionuclide concentrations, an atomic absorption spectrometry (AAS) was used to measure cesium and an inductively coupled plasma–optically emision spectrometry (ICP-OES) was used to measure strontium and rubidium. The spectrophotometer, namely model 7300DV, was produced by the Perkin Elmer Company. The recovery percent of the radionuclides was gained from Eq. (1).

$$R = \frac{C0 - C1}{C0} \times 100 \tag{1}$$

where C_0 and C_1 are for the strontium, cesium, and rubidium initial concentration in feed and their final concentration after adsorption in mg/l; R is their recovery percent.

2.3. Pilot System

To study the impact of the pollutant concentration, adsorbent concentration, and pH variables on the efficiency of the magmolecular process, 27 experiments were conducted in the pilot system; the schematic is represented in Figure 2. This system had two separate tanks, one for the feed (tank 1) and another for the adsorbent (tank 2) solutions. To perform the mixing of feed and adsorbent solutions, a contactor with a 130 rpm polyethylene mixer was installed in the system which was of a mixed stream type and had four blades. A solenoid valve was installed at the outlet of the contactor from which the solution was directed to the magnetic separator. The magnetic separator with a constant magnetic field of 1.2 Tesla was used to separate the ferritin molecules from the applied solution. It should be noted that all of the experiments were conducted at room temperature (25 °C).

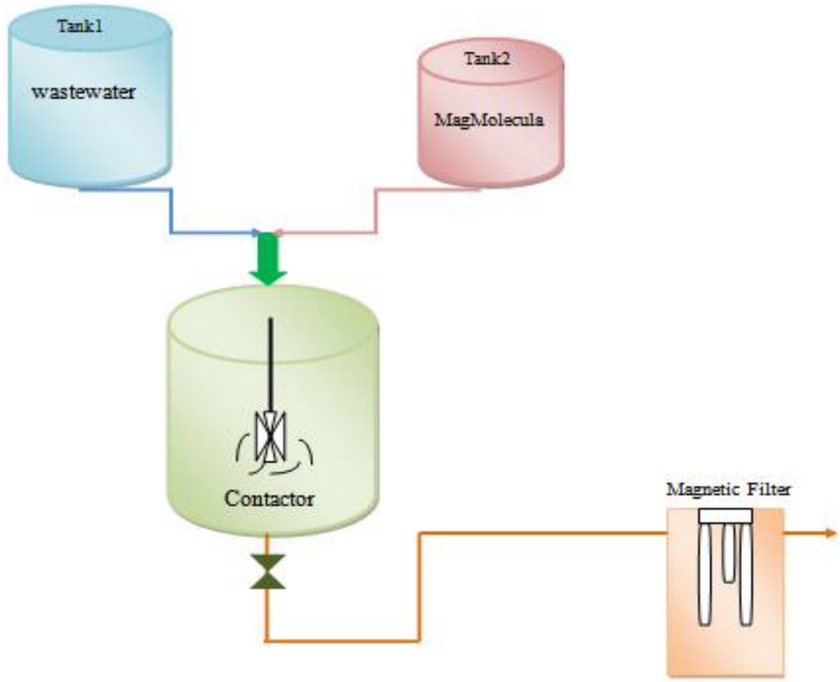

Fig. 2. The schematic of the designed magmolecular system

2.4. Experiments

This study employed Minitab 17 statistical software; the Taguchi method was applied to examine the adsorption process of cesium, strontium, and rubidium. The number of compounds may increase in processes which involve too many variables. A common way to decrease the number of experimental compounds is to use fractional factorial designs [16]. Taguchi creates a particular set of general designs for factorial designs that covers most applications. Orthogonal arrays are a part of these designs that significantly reduces the number of experiments, amount of time, and costs when compared to other statistical techniques [17]. In the Taguchi method, various 2-level, 3-level, 4-level, and 5-level designs with different variables are possible [18]. The control variables and their levels in this study are shown in Table 2. By means of the Taguchi method (L_9 orthogonal array), the experiments in this study were designed for three variables: metal pollutant concentration, adsorbent concentration, and pH with three levels (see Table 3). These three variables were the controlled factors and the recovery percent of cesium, strontium, and rubidium radionuclides were considered the response of the experiment. The assumed range of metal ion concentration was approximate to the actual and applicable concentrations. Due to its availability and price, the range of 0.011-0.00027 grams of the adsorbent per liters of the solution was selected for the ferritin. Also, as the initial pH of natural wastewater is usually around 7 and according to the range of pH used in most of the experiments, the range of pH was assumed to be 6-7.5 for this study. In previous studies, the variables of temperature, mixer rounds, and magnetic field did not have a significant impact on adsorption and therefore, they were assumed fixed at 25 °C, 130 rpm and 1.2 Tesla, respectively. According to the pretests, the time of 4 hours was close to equilibrium in most cases; therefore, this time was considered the experiment time in all of the experiments.

Table 2. Variables and levels of the magmolecular process

Variable	Symbol	Level 1	Level 2	Level 3
pollutant concentration (mg/l)	X_1	44.44	80	363.63
Adsorbent concentration (g/l)	X_2	0.011	0.002	0.00027
pH	X_3	6	7	7.5

3. Results and discussion

For the characterization of ferritin as a magmolecule, its FTIR spectra (Figure 3) is shown in the wavelength of 500-4000 cm^{-1}; the wavelength range of 3300-3750 is related to –OH of ferritin; the wavelength and 3000-2900 cm^{-1} is belong to -CH connected to –N and C=O; the wavelength of 2500 cm^{-1} is related to -CH connected to –C of bonded to –N, and -C=O. Also, the wavelength of 887-1156 cm^{-1} is for –CH of connected to –C of away from –N. According to the functional group of carboxylic acid in ferritin, the C=O bond is found in the wavelengths of 621-1030 and 3800-3900 cm^{-1}. Furthermore, the –NH group is present in the wavelength of 1267-1958 cm^{-1} [19].

Table 3. Design of the Taguchi method for the three independent variables

Run	Pollutant Concentration (mg/l); x_1	Adsorbent Concentration (g/l); x_2	pH; x_3
1	44.44	0.011	6
2	44.44	0.002	7
3	44.44	0.00027	7.5
4	80	0.011	7
5	80	0.002	7.5
6	80	0.00027	6
7	363.63	0.011	7.5
8	363.63	0.002	6
9	363.63	0.00027	7

According to the table of suggested experiment designs, the change in the amount of cesium, strontium, and rubidium adsorption with the change in the variables of pollutant concentration, adsorbent concentration, and pH for each experiment was computed from Equation 1. Then, the system's responses (recovery percent) were entered into the Minitab 17 software and the Taguchi analysis was run. Signal to noise (S/N) and variance analyses (ANOVA) were carried out to analyze the results. In fact, the signal to noise ratio showed the sensitivity of the system's response to uncontrollable and effective output factors in the process. The equation of computing signal to noise is defined in two conditions as follows [20]:

1. When the smaller value of "*y*" is indicative of the optimal level: Eq. (2) is used when the objective is to minimize the value of "*y*".

$$\frac{S}{N} = -10\log\frac{1}{n}\sum y^2 \tag{2}$$

2. When the greater value of "*y*" is indicative of the optimal level: Eq. (3) is used when the objective is to maximize the value of "*y*".

$$\frac{S}{N} = -10\log\frac{1}{n}\sum\frac{1}{y^2} \tag{3}$$

In the above equations "*n*" is the number of observations and "*y*" is the system's responses in the conducted experiments. Therefore, as it is desirable to maximize the recovery of cesium, strontium, and rubidium radionuclides, the level of variables which have the most degree of signal to noise were assumed as optimal levels. The signal to noise diagrams of cesium, strontium, and rubidium adsorption are shown in Figures 4, 5, and 6, respectively.

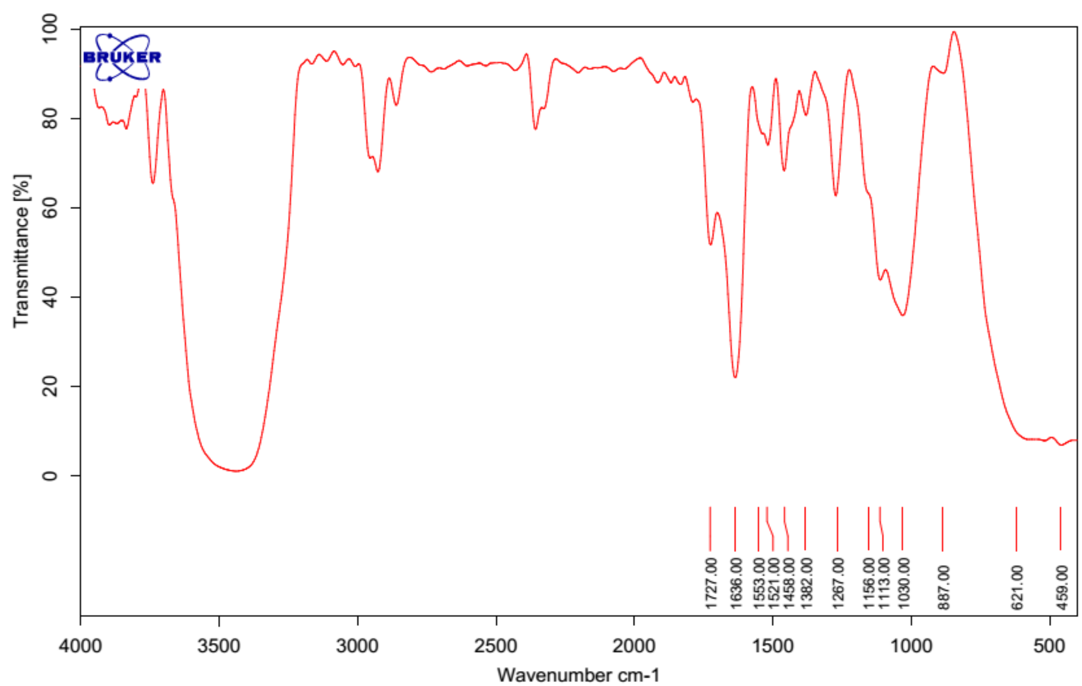

Fig. 3. FTIR analysis of the ferritin molecule before adsorption

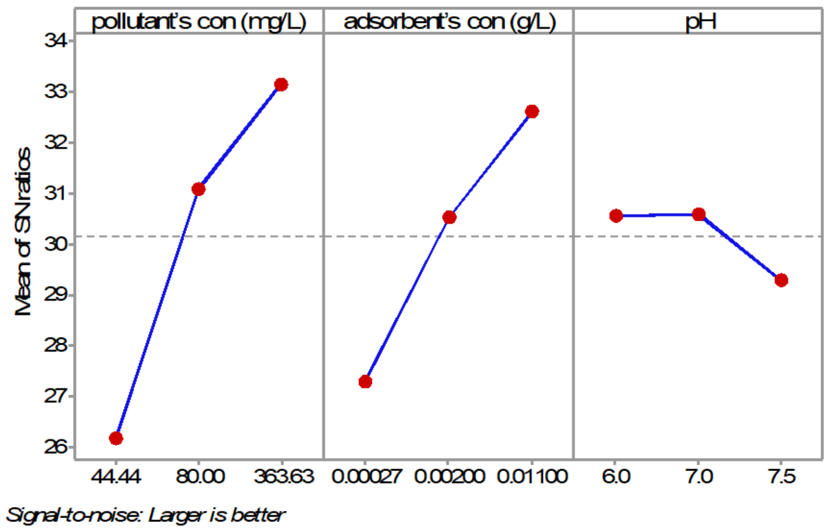

Fig. 4. Signal to noise diagram of cesium adsorption experiments related to the variables of pollutant concentration, adsorbent concentration, and pH

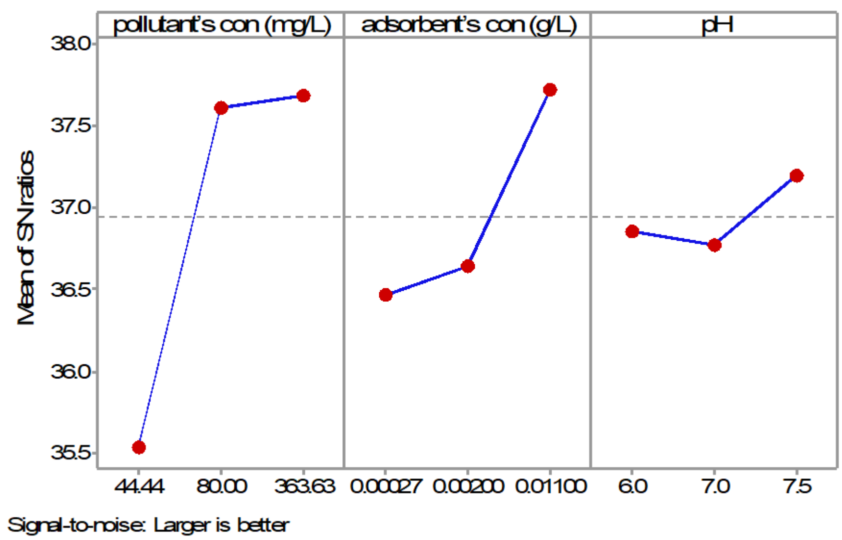

Fig. 5. Signal to noise diagram of strontium adsorption experiments related to the variables of pollutant concentration, adsorbent concentration, and pH

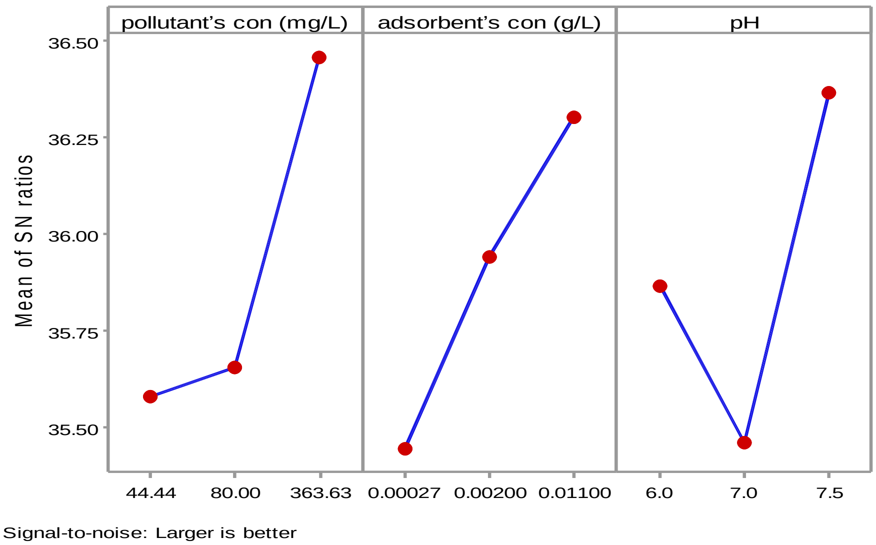

Fig. 6. Signal to noise diagram of rubidium adsorption experiments related to the variables of pollutant concentration, adsorbent concentration, and pH

According to these diagrams, the optimal conditions of adsorbing the three metal ions in the studied range were the pollutant concentration of 363.63 mg/l, adsorbent concentration of 0.011 g/l, and pH of 7-7.5. It was expected that the maximum recovery percent belong to the least concentration of pollutant, but in the present study, the maximum recovery occurred in the highest concentration of pollutant. The reason could be that in some ranges, with an increase in concentration, the environment's ionic strength undergoes some changes and this process may lead to the above mentioned phenomenon [21]. Furthermore, considering that the adsorbent concentration is indicative of the number of the adsorbent sites available for adsorbing, an increase in the adsorbent concentration results in the pollutant's wider access to the available sites and hence, the increase in the adsorption efficiency. In the cesium adsorption process through the 2-stage microfiltration technique, Han et al. reached a higher degree of adsorption by increasing the adsorbent's concentration [22]. It is obvious from the signal to noise diagram that the pH variable had a lesser impact on the adsorption process due to a gentler slope. Also, maximum adsorption occurred in neutral pHs (7.5 for strontium and rubidium, 7 for cesium). This took place because of the ferritin molecules more efficient performance in neutral pHs. Furthermore, as the pH decreased, the radionuclides with released protons (H^+) competed more aggresively to adsorb active sorption sites where "y" is the element's percent recovery, x_i is each variable, and β_i is the model's regression coefficient [21] and this in turn resulted in a lower adsorption rate. In another study, Torab Mosta'edi et al. found the optimal pH of 7 in the process of strontium and barium adsorption on the expanded perlite [23].

To measure the impact of each variable on the results and responses of the system, variance analysis of the results was carried out via the Minitab software. The general form of the linear model in the Taguchi method is as Eq. (4). Therefore, the fitting of the cesium, strontium, and rubidium adsorption data to Equation 4 would result in Eq. (5), Eq. (6), and Eq. (7), respectively. Also, the results of the variance analysis of cesium, strontium, and rubidium radionuclides are shown in Tables 4, 5, and 6, respectively.

$$y = \beta_0 + \sum_{i=1}^{3} \beta_i x_i \tag{4}$$

$$\% R_{Cs} = 7.9 + 0.0584 \times x_1 + 1379 \times x_2 + 1.7 \times x_3 \quad R^2 = 0.8703 \tag{5}$$

$$\% R_{Sr} = 45.2 + 0.0332 \times x_1 + 923 \times x_2 + 2.4 \times x_3 \quad R^2 = 0.8077 \tag{6}$$

$$\% R_{Rb} = 43.3 + 0.0221 \times x_1 + 533 \times x_2 + 1.95 \times x_3 \quad R^2 = 0.7422 \tag{7}$$

Table 4. The outcome of variance analysis of the results of cesium radionuclides adsorption tests from the synthetic solution

Variable	Coefficient	Standard error coefficient	T-value	p-value
Constant	7.9	33.8	0.23	0.824
pollutant concentration (mg/l)	0.0584	0.0213	2.74	0.041
adsorbent concentration (g/l)	1379	647	2.13	0.086
pH	1.7	4.88	0.35	0.742

Table 5. The outcome of variance analysis of the results of strontium radionuclides adsorption tests from the synthetic solution

Variable	Coefficient	Standard error coefficient	T-value	p-value
Constant	45.2	37.7	1.2	0.002
pollutant concentration (mg/l)	0.0332	0.0238	1.4	0.248
adsorbent concentration (g/l)	923	722	1.28	0.508
pH	2.4	5.44	0.44	0.839

Table 6. The outcome of variance analysis of the results of rubidium radionuclides adsorption tests from the synthetic solution

Variable	Coefficient	Standard error coefficient	T-value	p-value
Constant	43.3	20.3	2.13	0.086
pollutant concentration ($mg.l^{-1}$)	0.0221	0.0128	1.72	0.146
adsorbent concentration ($g.l^{-1}$)	533	390	1.37	0.230
pH	1.95	2.94	0.66	0.538

A standard error coefficient is used to understand the proximity of the sample mean to the population mean in the above tables. The standard error is calculated by dividing standard deviation on the root total number of samples. The smaller the standard error coefficient, the greater the accuracy of the predictive model. Also, the T-value is gained by dividing the predictive models' regression coefficients on the standard error coefficient. This test shows how close the selected samples of random variables are to the actual value (which the researcher does not know). The main logic behind calculating the p-value is to generalize the results to the whole population, but it does not reveal the degree or intensity of the difference between values; therefore, other tests such as T-value, F-value, and Z-value are used to calculate the difference. Also, the coefficient of determination (R^2) is a value in which the accuracy of the relationship between the independent and dependent variables is measured. The closer this value is to one, the smaller the error between the model and the experiment, hence, a more favorable regression. It was obvious from the resulting regression models that the coefficient of determinations of the three radionuclides were more than 0.74, and the best fitting between the model result and laboratory results was that of the cesium radionuclides. The adsorption rate was calculated using the regression models for the three radionuclides by replacing the designed variables in Table 3. The results indicated that the highest percent recovery for cesium, strontium, and rubidium was 57.05, 85.42, and 71.82, respectively, in the pollutant concentration of 363.63 mg/l, adsorbent concentration of 0.011 g/l, and pH of 7.5. Therefore, it can be understood that ferritin was more efficient in adsorbing divalent ions of strontium compared to univalent ions of cesium and rubidium in the magmolecular process. To determine the randomness of errors in a statistical regression, the errors can be presented according to the times the experiments were carried out. Figures 7, 8, and 9 show residual plots developed from the variance analysis of the cesium, strontium, and rubidium ions via the resulting linear models. The normal distribution of the residual (difference between the observed and the fitted values) should be studied. The assumption of being normal is usually investigated after drawing the normal probability curve according to the residual. Diagram (7a) represents the normal probability of the residuals resulting from the experiment's design, and the fact that these plots form a hypothetical line shows that the resulting error are random and they follow a normal population. Therefore, considering the random nature of the resulting errors, the model's accuracy is confirmed. Diagram (7b) showing the residual according to the fitted values, confirms an acceptable random distribution around the zero axis and shows that standard deviation for any observation compared to another observation falls within the range of -2 to +2. Diagram (7d) shows that the residuals are randomly distributed according to the observations and do not follow a definite pattern; therefore, there are no systematic errors in the experiments.

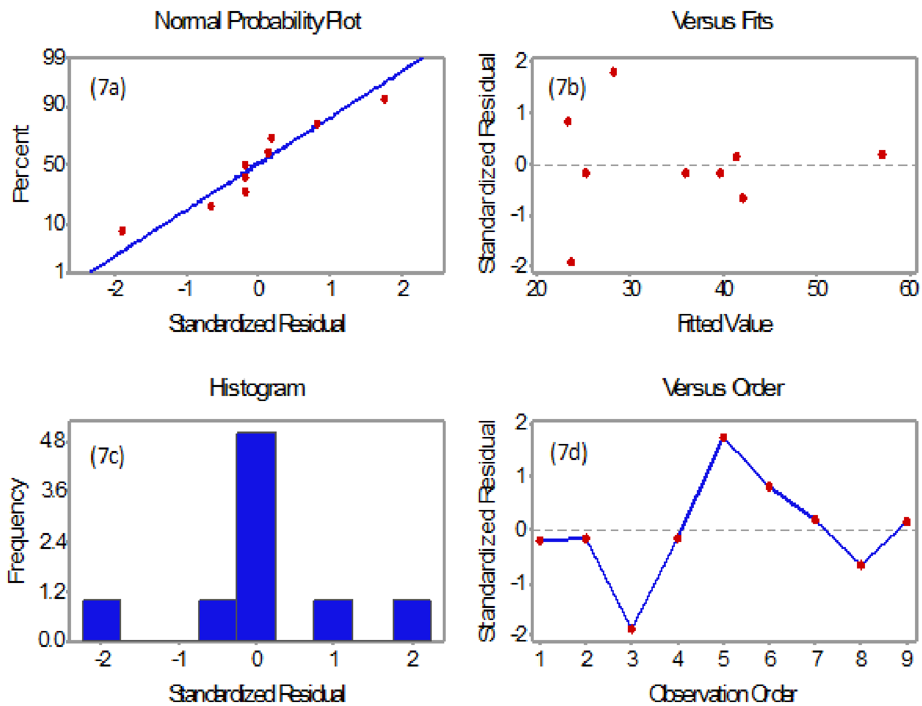

Fig. 7. Residual plots resulting from variance analysis of cesium radionuclides a) normal probability function b) residual plot according to the fitting cure c) each variable's frequency diagram d) residual plots according to the observations

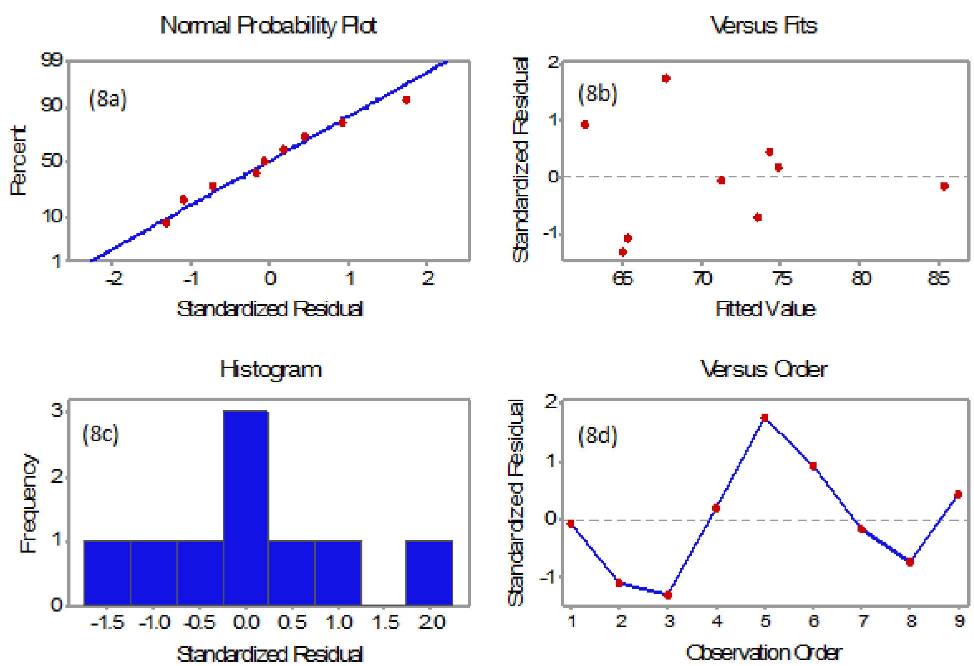

Fig. 8. Residual plots resulting from variance analysis of strontium radionuclides a) normal probability function b) residual plot according to the fitting cure c) each variable's frequency diagram d) residual plots according to the observations

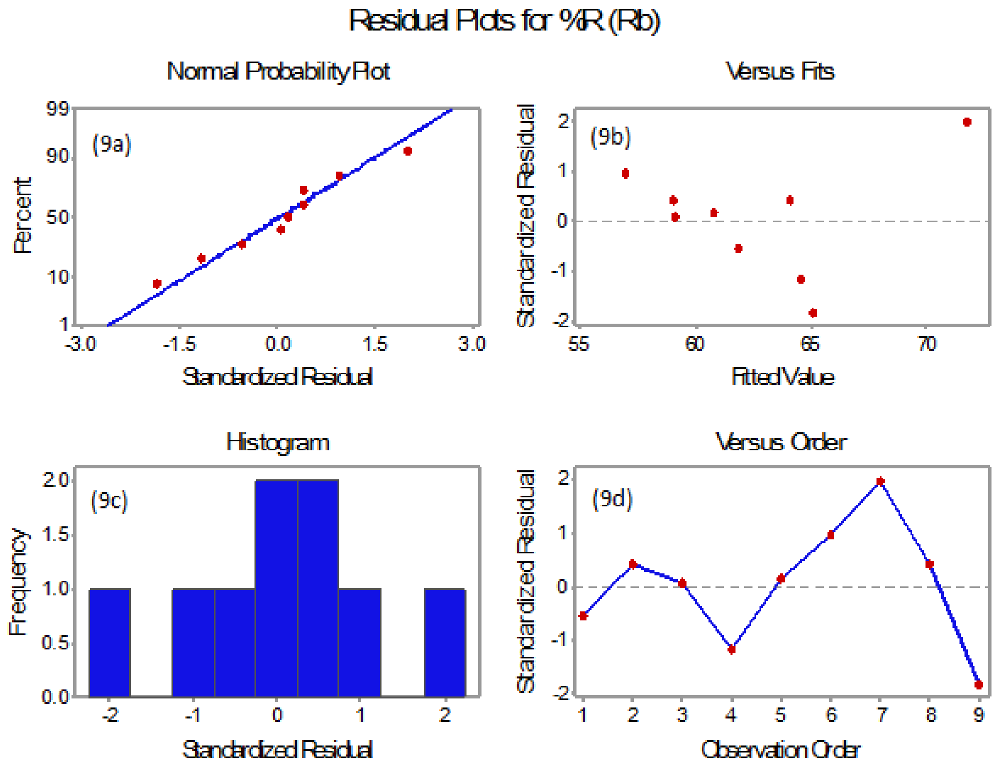

Fig. 9. Residual plots resulting from variance analysis of rubidium radionuclides a) normal probability function b) residual plot according to the fitting cure c) each variable's frequency diagram d) residual plots according to the observations

By comparing the residual plots of cesium, strontium, and rubidium radionuclides, it can be understood that error distribution in the predicted model (difference of laboratory values and values obtained from the model) for cesium radionuclides is higher than other radionuclides.

4. Conclusions

In this study, the adsorption of cesium, strontium, and rubidium radionuclides by ferritin magmolecules in a batch system was investigated. To reduce experimental costs and time, the Taguchi method of designing was adopted with 9 experiments for each radionuclide. Variance and signal to noise analyses were run on the results via Minitab software to determine the impact of each variable on the results and system responses. The study of the p-value (related to adsorbtion of cessium) showed that the concentration of the adsorbent and pollutant were more effective parameters than pH. Also, the concentration of the adsorbent and pollution had a maximum variation of signal to noise ratio. In regard to strontium, pollutant concentration had the minimum p-value and maximum variation of signal to noise ratio (Figure 5). Furthermore, the p-value equal to 0.002 for constant showed that other parameters, besides those that have been investigated here, were effective in the strontium magmolecular process. This explanation was also valid for rubidium adsorption (Figure 6). Using the offered regression models, the highest percent recovery in the studied range was 57.05, 85.42, and 71.82 for cesium, strontium, and rubidium radionuclides, respectively, when the pollutant concentration was 363.63 mg/l, adsorbent concentration was 0.011 g/l and pH was 7.5. Therefore, it could be understood that the ferritin adsorbent in the magmolecular process manifested a higher efficiency in adsorbing bivalent ions of strontium compared to univalent ions of cesium and rubidium. Fitting the results to the regression linear model resulted in relationships between the independent variables and a percent recovery (dependent variable) with a coefficient of determination of 0.8703, 0.8077, and 0.7422 for cesium, strontium, and rubidium, respectively. These models are valid for this study domain.

References

[1] Anzai, K., Ban, N., Ozawa, T., Tokonami, S. (2012). Fukushima Daiichi Nuclear Power Plant accident: facts, environmental contamination, possible biological effects, and countermeasures. *Journal of clinical biochemistry and nutrition*, *50*(1), 2-8.

[2] Liu, X., Chen, G. R., Lee, D. J., Kawamoto, T., Tanaka, H., Chen, M. L., Luo, Y. K. (2014). Adsorption removal of cesium from drinking waters: A mini review on use of biosorbents and other adsorbents. *Bioresource technology*, *160*, 142-149.

[3] Munthali, M. W., Johan, E., Aono, H., Matsue, N. (2015). Cs^+ and Sr^{2+} adsorption selectivity of zeolites in relation to radioactive decontamination. *Journal of Asian ceramic societies*, *3*(3), 245-250.

[4] Moamen, O. A., Ismail, I. M., Abdelmonem, N., Rahman, R. A. (2015). Factorial design analysis for optimizing the removal of cesium and strontium ions on synthetic nano-sized zeolite. *Journal of the Taiwan institute of chemical engineers*, *55*, 133-144.

[5] Kamaraj, R., Vasudevan, S. (2015). Evaluation of electrocoagulation process for the removal of strontium and cesium from aqueous solution. *Chemical engineering research and design*, *93*, 522-530.

[6] Ye, X., Wu, Z., Li, W., Liu, H., Li, Q., Qing, B., Ge, F. (2009). Rubidium and cesium ion adsorption by an ammonium molybdophosphate–calcium alginate composite adsorbent. *Colloids and surfaces A: Physicochemical and engineering aspects*, *342*(1), 76-83.

[7] Yakout, S. M., Hassan, H. S. (2014). Adsorption characteristics of sol gel-derived zirconia for cesium ions from aqueous solutions. *Molecules*, *19*(7), 9160-9172.

[8] Khotimchenko, M. Y., Podkorytova, E. A., Kovalev, V. V., Khozhaenko, E. V., Khotimchenko, Y. S. (2014). Removal of cesium from aqueous solutions by sodium and calcium alginates. *Journal of environmental science and technology*, *7*(1), 30-43.

[9] Guerra, D. L., Batista, A. C., Viana, R. R., Airoldi, C. (2011). Adsorption of rubidium on raw and MTZ-and MBI-imogolite hybrid surfaces: An evidence of the chelate effect. *Desalination*, *275*(1), 107-117.

[10] Warner, C. L., Addleman, R. S., Cinson, A. D., Droubay, T. C., Engelhard, M. H., Nash, M. A., Warner, M. G. (2010). High-Performance, Superparamagnetic, nanoparticle-based heavy metal sorbents for removal of contaminants from natural waters. *ChemSusChem*, *3*(6), 749-757.

[11] Galvez, N., Fernandez, B., Sanchez, P., Cuesta, R., Ceolin, M., Clemente-Leon, M., Trasobares, D., Lopez-Haro, M., Calvino, J. J., Stephan, O., Dominguez-Vera, J. M. (2008). Comparative structural and chemical studies of ferritin cores with gradual removal of their iron contents. *Journal of the American chemical society*, 130(25), 8062–8068.

[12] Harrison, P. M., Arosio, P. (1996). The ferritins: molecular properties, iron storage function and cellular regulation. *Biochimica et biophysica acta (BBA)-bioenergetics*, *1275*(3), 161-203.

[13] Rooygar, A. A., Mallah, M. H., Abolghasemi, H., Safdari, J. (2014). New “magmolecular” process for the separation of antimony (III) from aqueous solution. *Journal of chemical and engineering data*, *59*(11), 3545-3554.

[14] Nabavi Larimi, Y., Mallah, M. H., Moosavian, M. A., Safdari, J. (2016). Kinetic and equilibrium study of selenium removal from wastewater in mag-molecular process. *Desalination and water treatment*, *57*(2), 933-948.

[15] Bushart, S. P., Bradbury, D., Elder, G., Duffield, J., Pascual, I., Ratcliffe, N. (2006, July). The development of magnetic molecules for the selective removal of contaminants. In *waste management conference*.

[16] Antony, J. (2003). Design of experiments for engineers and scientists, First Ed., Elsevier, pp. 73-93.

[17] Kuram, E., Ozcelik, B. (2013). Multi-objective optimization using Taguchi based grey relational analysis for micro-milling of Al 7075 material with ball nose end mill. *Measurement*, *46*(6), 1849-1864.

[18] Kavand, M., Kaghazchi, T., Soleimani, M. (2014). Optimization of parameters for competitive adsorption of heavy metal ions (Pb, Ni, Cd) onto activated carbon. *Korean journal of chemical engineering*, *31*(4), 692-700.

[19] Zhang, L. (2011). Interaction of Ferritin with transition metal ions and chelates. PhD Dissertation. University of Pennsylvania.

[20] Santangelo, S., Messina, G., Malara, A., Lisi, N., Dikonimos, T., Capasso, A Faggio, G. (2014). Taguchi optimized synthesis of graphene films by copper catalyzed ethanol decomposition. *Diamond and related materials*, *41*, 73-78.

[21] Mansoorian, H. J., Mahvi, A. H., Mostafapoor, F. K., Alizadeh, M. (2013). Equilibrium and synthetic studies of methylene blue dye removal using ash of walnut shell. *Journal of health in the field*, *1*(3), 48-55.

[22] Han, F., Zhang, G. H., Gu, P. (2012). Removal of cesium from simulated liquid waste with countercurrent two-stage adsorption followed by microfiltration. *Journal of hazardous materials*, *225*, 107-113.

[23] Torab-Mostaedi, M., Ghaemi, A., Ghassabzadeh, H., Ghannadi-Maragheh, M. (2011). Removal of strontium and barium from aqueous solutions by adsorption onto expanded Perlite. *The Canadian journal of chemical engineering*, *89*(5), 1247-1254.